ISBN: 978-3-95450-232-5 ISSN: 2673-7000 doi:10.18429/JACoW-NAPAC2022-WEPA02

BEAM DYNAMICS STUDIES ON A LOW EMITTANCE INJECTOR FOR LCLS-II-HE *

F. Ji†, C. E. Adolphsen, C. Mayes, T. O. Raubenheimer, R. Coy, L. Xiao, L. Ge
SLAC National Accelerator Laboratory, Menlo Park, CA, USA
J. Qiang, Lawrence Berkeley National Laboratory, Berkeley, CA, USA

Abstract

The SLAC High Energy upgrade of LCLS-II will double the beam energy to 8 GeV, increasing the XFEL photon energy reach to about 13 keV. The energy reach can be extended to 20 keV if the beam emittance can be halved, which requires a higher gradient electron gun with a lower intrinsic emittance photocathode. To this end, the Low Emittance Injector (LEI) will be built that will run parallel to the existing LCLS-II Injector. The LEI design will be based on a state-of-the-art SRF gun with a 30 MV/m cathode gradient. The main goal is to produce transverse beam emittances of 0.1 mm-mrad for 100 pC bunch charges. This paper describes the beam dynamics studies on the design of the LEI including the simulations and multi-objective genetic algorithm optimizations. Performance with different injector layouts, cathode gradients and bunch charges are presented.

INTRODUCTION

X-ray Free Electron Lasers (XFELs) provide ultrafast coherent X-ray pulses for the study of structural dynamics on atomic spatial (Å) and time (fs) scales [1]. Such measurements provide critical insights into the fundamental processes in complex functional materials, gas phase molecules and biological systems [2]. The LCLS-II High Energy Upgrade (LCLS-II-HE) is a 4 GeV extension of the LCLS-II SRF linac that increases the high repetition rate XFEL photon energy reach from 5 keV to 13 keV [3]. The photon spectral range can be extended to 20 keV if the beam emittance can be halved. To this end, a Low Emittance Injector (LEI) will be built that will run parallel to the existing LCLS-II injector. The LEI design is based on a state-of-the-art 185.7 MHz, quarter-wave resonator (QWR) type Superconducting RF (SRF) gun [4] with a 30 MV/m cathode gradient. The goal is to produce 100 pC bunches with transverse emittances of 0.1 mm-mrad and lengths of σ_z = 1 mm (corresponding to 10 A peak current). In this paper, we describe the injector design optimization and performance with different injector layouts, cathode gradients and bunch charges.

INJECTOR OPTIMIZATION OVERVIEW

The strategy to achieve low emittance is to use both a higher cathode gradient and a lower Mean Transverse Energies (MTE) photocathode than those in LCLS-II [5, 6]. A MSU-ANL-HZDR collaboration is building a prototype QWR type SRF gun based on a cavity design developed at SLAC for this application [4]. The initial goal is to achieve stable operation with a metal cathode plug for cathode gradients up to 30 MV/m. Based on experience with Alkali Antimonide photocathodes illuminated with green laser light, a MTE of 184 meV (i.e., intrinsic emittance = 0.6 μm/mm) was chosen as the working assumption for the LEI emittance optimization studies.

Once the beam is generated in the gun, space charge forces induce a bunch slice phase space mismatch that can cause transverse emittance degradation downstream. The standard approach for compensating such emittance degradation is to use a set of solenoids to rotate the slices differentially to re-align them downstream (i.e., emittance compensation [7]). To this end, a compact ferrite-based solenoid was simulated and the solenoid to cavity anode distance was optimized for emittance compensation. To better optimize the emittance over a range of cathode gradients and bunch charges, two sets of windings were included that could be independently powered so that both the solenoid strength and magnetic centroid could be varied.

Figure 1 illustrates two LEI configurations that were evaluated. The Compact configuration includes an SRF gun, gun solenoid, buncher cavity, second solenoid and an LCLS-II-HE type cryomodule (CM). The compact layout is similar to the LCLS-II injector except that a 9-cell SRF cavity is used for bunching, which allows a voltage gain of up to 16 MV. Although the resulting emittance was acceptable, the optimized layout left little space between the gun and the buncher, and as discussed below, the emittance grew rapidly at lower gradients. The Complex layout utilizes a two stage bunching strategy: an LCLS-II type normal conducting (NC) buncher and solenoid are included between the gun solenoid and the 9-cell buncher. The NC buncher is located 0.91 m from cathode, which allows the 9-cell buncher to be located 3.4 m from cathode, freeing up space for a full LCLS-II like diagnostic section. As an alternative, an LEI configuration without a buncher has been explored [8].

For both Compact and Complex configurations, the performance was evaluated with cathode gradients of 20 and 30 MV/m and bunch charges of 25, 100 and 200 pC. The cathode MTE was fixed at 184 meV and 10,000 macro particles were used when running the Multi-Object Genetic Algorithm(MOGA) NSGA-II code. The z locations of the beamline components were fixed for this study and were set to the optimized values for a 30 MV/m gradient and 100 pC charge. Table 1 lists the parameters that were varied and their ranges during MOGA optimizations.

* Work supported by U.S. Department of Energy Office of Science, Basic Energy Sciences under Contract No. DE-AC02-76SF00515.
† fuhaoji@slac.stanford.edu

ISBN: 978-3-95450-232-5 ISSN: 2673-7000 doi:10.18429/JACoW-NAPAC2022-WEPA02

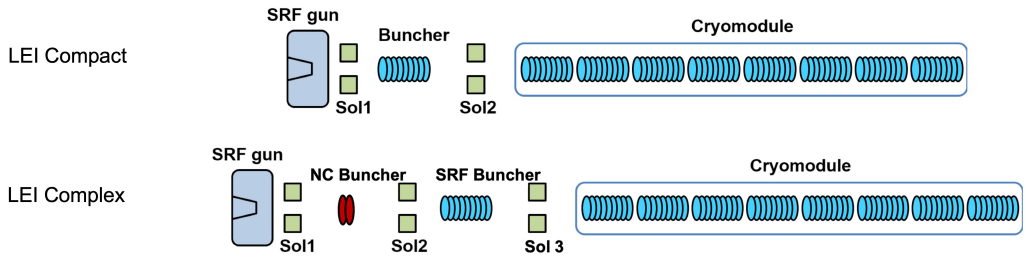

Figure 1: Low Emittance Injector layout options.

Particle tracking codes with space charge algorithms were utilized to perform the beam dynamics simulations. These include ASTRA [9] and Impact-T [10]. Also, the Lightsource Unified Modeling Environment(LUME) [11] was utilized, which greatly improved the efficiency of the beam dynamics simulations and optimizations. All simulations were performed on the supercomputer Cori at the high-performance computation user facility NERSC. The output for every evaluation was archived in a standard format.

OPTIMIZATION RESULTS

The NSGA-II optimization algorithm is capable of evaluating trade-offs between competing objectives and the result is a population of solutions, which is referred to as a Pareto Front. Figure 2 illustrates a typical set of optimization results where the horizontal axis is the rms bunch length at the end of the CM and the vertical axis is the 95% normalized emittance. The orange and blue curves show the Pareto Fronts corresponding to the Complex configuration for 100 pC bunches with 30 MV/m and 20 MV/m cathode gradients, respectively. Solutions corresponding to σ_z = 1 mm are highlighted using stars. The emittance values are 0.093 µm at 30 MV/m and 0.110 µm at 20 MV/m, which clearly demonstrates the benefit of Complex layout in accommodating lower gradients.

Table 1: Beam dynamics optimization parameters and ranges.

Parameter	Range	Unit
Gun phase	[−15, 15]	degree
Gun solenoid strength	[0.01, 0.18]	T
NC buncher amplitude	[2.0, 3.0]	MV/m
NC buncher phase	[−90, −40]	degree
Solenoid 2 strength	[0.01, 0.15]	T
9-cell buncher amplitude	[1, 32]	MV/m
9-cell buncher phase	[−90, -40]	degree
Solenoid 3 strength	[0.01, 0.15]	T
CM cavity 1-4 amplitude	[1, 32]	MV/m
CM cavity 1-4 phase	[−60, 60]	degree
CM cavity 5-8 amplitude	[20, 32]	MV/m
CM cavity 5-8 phase	[−20, 20]	degree
Laser spot size	[0.05, 2.00]	mm
Laser FWHM pulse length	[10, 60]	ps

In a similar comparison for the Compact configuration, an emittance of 0.10 µm could be achieved at 30 MV/m, but at 20 MV/m, the emittance is 0.40 µm, which would not meet the LCLS-II-HE requirement.

To improve the Compact performance at 20 MV/m, a gun geometry with a larger cathode-to-anode gap (9 cm vs. 7 cm) was considered as higher beam energy was seen to lower space charge force and emittance. Other layout changes were also explored for both Compact and Complex layouts including (1) moving the 9-cell buncher further downstream to provide more space between the gun and buncher cryomodule and (2) lowering the NC buncher field, which would reduce its heat load. Table 2 lists optimization results for various cases with these changes. With the 9 cm gap, the Compact performance improves considerably at 20 MV/m (Case 5), but the 100 pC emittance would still be as large as that in the LCLS-II injector if it could operate with MTE = 184 meV cathodes, and the emittance is very sensitive to the z location of the 9-cell buncher (compare case 5 and 6). The Complex results are much less sensitive to the 9-cell buncher z location and are fairly insensitive to a reduction in the NC buncher field strength. At other gradients and bunch charges, the Complex (Case 2) and Compact (Case 5) emittances are similar.

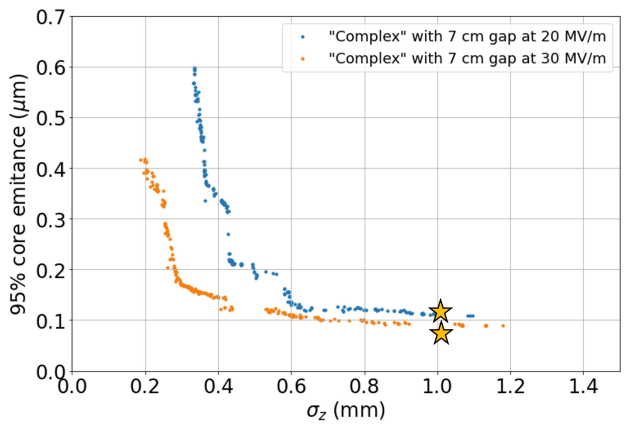

Figure 2: Emittance vs. bunch length Pareto Front corresponding to the Complex layout at 30 MV/m and 20 MV/m cathode gradients for a bunch charge of 100 pC.

ISBN: 978-3-95450-232-5 ISSN: 2673-7000 doi:10.18429/JACoW-NAPAC2022-WEPA02

Table 2: Optimized 95% normalized emittance at σ_z = 1 mm for the Compact and Complex layouts for different configurations. $Z_{9\text{-cell}}$ is the 9-cell buncher location, E_{NC} is the NC buncher amplitude and the gun cavity gap is 7 cm unless otherwise noted.

Case	Configuration	30 MV/m, 100 pC	20 MV/m, 100 pC	30 MV/m, 200 pC	30 MV/m, 25 pC	20 MV/m, 25 pC
1	Complex $Z_{9\text{-cell}}$ = 3.4 m E_{NC} = 2.5 MV/m	0.094 µm	0.128 µm	0.149 µm	0.049 µm	0.065 µm
2	Complex $Z_{9\text{-cell}}$ = 3.4 m E_{NC} = 3.0 MV/m	0.092 µm	0.110 µm	0.154 µm	0.047 µm	0.057 µm
3	Complex $Z_{9\text{-cell}}$ = 3.7 m E_{NC} = 2.5 MV/m	0.092 µm	0.156 µm	0.191 µm	0.047 µm	-
4	Compact $Z_{9\text{-cell}}$ = 2.5 m	0.094 µm	0.402 µm	0.148 µm	-	-
5	Compact $Z_{9\text{-cell}}$ = 2.5 m Gun gap = 9 cm	0.086 µm	0.168 µm	0.153 µm	0.048 µm	0.067 µm
6	Compact $Z_{9\text{-cell}}$ = 3.0 m Gun gap = 9 cm	0.136 µm	0.373 µm	-	-	-

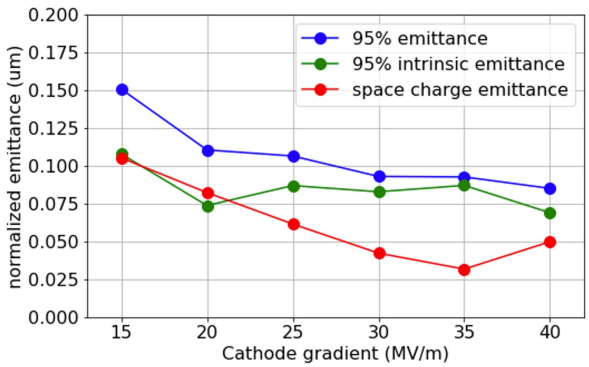

Figure 3: Optimized 95% normalized emittance at σ_z = 1 mm for the Complex configuration versus cathode gradient.

EMITTANCE VS. CATHODE GRADIENT

As discussed above, the cathode gradient has a large effect on the resulting beam brightness. However, operation may be limited to lower gradients due to dark current, which increases exponentially with gradient. This prompted further studies of the Complex configuration performance over a wider range of gradients, from 15 MV/m to 40 MV/m. Figure 3 illustrates the optimized emittance at σ_z = 1 mm versus cathode gradient where the cathode MTE was fixed at 184 meV. One can clearly see that the emittance trends downward with higher cathode gradient: a 95% emittance of 0.085 µm could be achieved with a cathode gradient of 40 MV/m. At 15 MV/m, the 95% emittance is 0.150 µm, which would still outperform the LCLS- II injector where the cathode gradient is 20 MV/m. Assuming that the final bunch emittance is the sum in quadrature of the intrinsic contribution and that from space charge effects, the latter component can be deconvolved. As shown in Figure 3, the space charge contribution decreases with higher cathode gradient, and flattens out for gradients > 30 MV/m.

CONCLUSION

The LCLS-II-HE project is a 4 GeV extension of the LCLS-II SRF linac that could increase XFEL photon energy reach up to 20 keV if the beam emittance can be halved relative to that in LCLS-II. To this end, a low emittance injector will be built that will run parallel to the existing LCLS-II injector. A state-of-the-art QWR type SRF gun will be used with the goal of delivering 100 pC bunches with 0.1 mm-mrad transverse emittances. Different injector layout options have been explored and the studies show that the desired beam emittance can be achieved with both 20 MV/m and 30 MV/m cathode gradients. The performance of the Complex injector configuration is relatively insensitive to buncher locations and field amplitudes compared to the Compact layout.

ACKNOWLEDGEMENTS

We thank R. Li and B. Legg for help setting up the simulations and useful discussions. This work was supported by the U.S. Department of Energy Office of Science, Office of Basic Energy Sciences under Contract No. DE-AC02-76SF00515. This research used resources of the National Energy Research Scientific Computing Center (NERSC), a U.S. Department of Energy Office of Science User Facility located at Lawrence Berkeley National Laboratory, operated under Contract No. DE-AC02-05CH11231 using NERSC award BES-ERCAP0016827 for 2021.

ISBN: 978-3-95450-232-5 ISSN: 2673-7000 doi:10.18429/JACoW-NAPAC2022-WEPA02

REFERENCES

[1] C. Bostedt, S. Boutet, D. M. Fritz, *et al.*, "Linac Coherent Light Source: The first five years", *Rev. Mod. Phys.*, vol. 88, p. 015007, 2016. doi:10.1103/RevModPhys.88.015007

[2] J. C. Hemminger, "Challenges at the Frontiers of Matter and Energy: Transformative Opportunities for Discovery Science", *BESAC Report*, Dep. Energy, 2015. doi:10.2172/1283188

[3] T. O. Raubenheimer, "The LCLS-II-HE, A High Energy Upgrade of the LCLS-II", in *Proc. FLS'18*, Shanghai, China, Mar. 2018, pp. 6–11. doi:10.18429/JACoW-FLS2018-MOP1WA02

[4] J. W. Lewellen *et al.*, "Status of the SLAC/MSU SRF Gun Development Project", presented at NAPAC'22, Albuquerque, NM, USA, Aug. 2022, paper WEPA03, this conference.

[5] I. V. Bazarov, B. M. Dunham, and C. K. Sinclair, "Maximum Achievable Beam Brightness from Photoinjectors", *Phys. Rev. Lett.*, vol. 102, p. 104801, 2009. doi:10.1103/PhysRevLett.102.104801

[6] D. Filippetto, P. Musumeci, M. Zolotorev, and G. Stupakov, "Maximum current density and beam brightness achievable by laser-driven electron sources", *Phys. Rev. Accel. Beams*, vol. 17, p. 024201, 2014. doi:10.1103/PhysRevLett.102.104801

[7] B. E. Carlsten, "Space-Charge-Induced Emittance Compensation in High-Brightness Photoinjectors", *Part. Accel.*, vol. 49, pp. 27-65, 1995.

[8] J. Qiang, F. Ji, and T. O. Raubenheimer, "Beam Dynamics Optimization of a Low Emittance Photoinjector Without Buncher Cavities", presented at NAPAC'22, Albuquerque, NM, USA, Aug. 2022, paper WEPA01, this conference.

[9] ASTRA – A Space-charge Tracking Algorithm, http://www.desy.de/~mpyflo/

[10] J. Qiang, S. Lidia, R. D. Ryne, and C. Limborg-Deprey, "Three-dimensional quasistatic model for high brightness beam dynamics simulation", *Phys. Rev. ST Accel. Beams*, vol. 9, p. 044204, 2006. doi:10.1103/PhysRevSTAB.9.044204

[11] C. E. Mayes *et al.*, "Lightsource Unified Modeling Environment (LUME), a Start-to-End Simulation Ecosystem", in *Proc. IPAC'21*, Campinas, Brazil, May 2021, pp. 4212–4215. doi:10.18429/JACoW-IPAC2021-THPAB217